Chinese Journal of Aeronautics, (2016), 29(1): 268–273

Chinese Society of Aeronautics and Astronautics
& Beihang University

Chinese Journal of Aeronautics

cja@buaa.edu.cn
www.sciencedirect.com

Ultrasound assisted solidification process of ternary Cu–Sn–Sb alloy

Zhai Wei, Hong Zhenyu, Liu Haiman, Wei Bingbo *

Department of Applied Physics, Northwestern Polytechnical University, Xi'an 710072, China

Received 7 September 2015; revised 12 October 2015; accepted 15 October 2015
Available online 30 October 2015

KEYWORDS

Copper alloys;
Mechanical property;
Microstructural evolution;
Peri-eutectic;
Power ultrasound

Abstract It is well-known that the application of ultrasound during liquid to solid transitions for alloys can refine the solidification microstructure and thus improves the mechanical properties. However, most published work focuses on single phase dendritic growth, whereas little has been conducted on the multiphase alloys with complicated phase transformations during solidification. In this work, the solidification process of ternary $Cu_{40}Sn_{45}Sb_{15}$ alloy was realized within intensive ultrasonic field with a resonant frequency of 20 kHz and ultrasound power from 0 W to 1000 W. The ultrasound refines the size of the primary ε(Cu_3Sn) intermetallic compound by two orders of magnitudes. If the ultrasound power increases to 1000 W, η(Cu_6Sn_5) phase nucleates and grows directly from parent liquid phase without the occurrence of peri-eutectic reaction on the top of the alloy sample where the ultrasound intensity is sufficiently high. These microstructural variations lead to the enhancement of compressive strength and elasticity modulus of ternary $Cu_{40}Sn_{45}Sb_{15}$ alloy.

1. Introduction

The microstructures of aerospace materials determine their applied properties. The solidification process of light alloys and superalloys for aerospace industries can be improved by ultrasound.[1–4] Thus the solidification of alloys within ultrasonic field has been an important research subject in recent years. The propagation of ultrasonic wave not only transmits acoustic energy into the liquid alloy, but also brings about such nonlinear effects as cavitation and acoustic streaming, which greatly affect the solidification process of alloys and ultimately improve their microstructures and mechanical properties.[5–8] So far, most work is focused on the dendritic growth of Al-based alloys[9–12] and Mg-based alloys[13–17] because of their wide applications in the automotive and aerospace industries.[18,19]

The peri-eutectic transition $L + \alpha \rightarrow \beta + \gamma$ is a typical kind of peritectic transformation in ternary and multicomponent alloys. Like the usual peritectic transition $L + \alpha \rightarrow \beta$, its reactants involve one liquid phase and one solid phase. However, its products are two cooperative solid phases. Since peri-eutectic transformation is an atomic diffusion controlled process which is difficult to be completed, the final microstructures are always composed of both primary and peri-eutectic phases.[20] Therefore, to control phase selection during peri-eutectic solidification is of great significance. However, the research of ultrasonic solidification of ternary

* Corresponding author.
Peer review under responsibility of Editorial Committee of CJA.

ELSEVIER Production and hosting by Elsevier

http://dx.doi.org/10.1016/j.cja.2015.10.014

peri-eutectic alloy is rather scarce. It can be speculated that if ultrasound is introduced into the solidification process of peri-eutectic alloy melt, the cavitation effect introduced by intensive ultrasound may alter the competitive nucleation between primary and peri-eutectic phases. Meanwhile, the acoustic streaming accelerates the solute transportation process, which may facilitate the peri-eutectic transformation.

Ternary Cu–Sn–Sb alloy is a complex metallic system whose solidification process involves multiple peri-eutectic transitions among various Cu–Sn, Sn–Sb and Cu–Sb intermetallic compounds. This makes it a good candidate of soldering materials without the toxic Pb element, because the formation of various intermetallic compounds could induce a significant composite strengthening effect, and thus has great potential applications in electronic interconnections of packing technology and automotive industry. In this work, the intense ultrasonic field is introduced into the solidification process of ternary $Cu_{40}Sn_{45}Sb_{15}$ alloy to investigate the microstructural evolution and mechanical property versus ultrasound power. On the basis of the experimental results, the peri-eutectic solidification mechanism is discussed.

2. Materials and method

The experiments were performed with a solidification apparatus incorporated with ultrasonic generator. The ternary $Cu_{40}Sn_{45}Sb_{15}$ alloy sample was ∅25 mm × 25 mm in size and was prepared from pure Cu (99.99%), Sn (99.99%) and Sb (99.99%) elements by using electrical resistance furnace. During the experiment, the alloy sample was melted by an electrical resistance furnace in the flowing argon atmosphere. The ultrasonic generator consists of two parts: a $KNbO_3$ piezoelectric transducer with a resonant frequency of 20 kHz and an ultrasonic horn with an end diameter of ∅22 mm. During experiment, the temperature was monitored by positioning a NiCr–NiSi thermocouple at the alloy sample top. When the alloy melting temperature dropped to 100 K above its liquidus temperature, the ultrasonic transducer was turned on and longitudinal ultrasonic wave was introduced from the top of the sample downward into the melted alloy until it solidified completely. Different exciting currents were input to the ultrasonic transducer. The corresponding ultrasound power P_W was estimated to be 250, 500, 1000 W. After experiments, the alloys samples were vertically sectioned, mounted, polished and etched. The phase constitution and microstructure of solidified alloy samples were analyzed by X-ray diffractometer (XRD) and scanning electron microscope (SEM).

The compression performance of ternary $Cu_{40}Sn_{45}Sb_{15}$ alloy was tested by CSS44100 universal electronic testing machine. Specimens in a size of ∅4.0 mm × 4.0 mm were cut from the central part of each alloy sample solidified with different ultrasound powers, and the loading speed of mechanical testing machine was set to be 0.3 mm/min downward. To ensure the accuracy of test results, the compression without samples was also conducted to make a baseline correction of machine-stiffness.

3. Results and discussion

3.1. Acoustic field distribution within liquid alloy

The sound distribution within liquid $Cu_{40}Sn_{45}Sb_{15}$ alloy is calculated by COMSOL Multi-physics 5.0 software. The propagation of ultrasound within liquid can be expressed by Helmholtz equation:

$$\frac{k^2}{\rho_0}p_a + \nabla \cdot \left(\frac{1}{\rho_0}\nabla p_a\right) = 0 \tag{1}$$

in which p_a is the sound pressure, $\rho_0 = 7746\ \mathrm{kg/m^3}$ the density of ternary liquid $Cu_{40}Sn_{45}Sb_{15}$ alloy, $k = \omega/c_0$ the wave number, $\omega = 2\pi f$, $c_0 = 3750\ \mathrm{m/s}$ the sound velocity, and $f = 20\ \mathrm{kHz}$ the resonant frequency of ultrasound. The acoustic initial and boundary conditions are set as follows: (a) pressure source $p_a = p_0\cos(\omega t)$ at the ultrasonic probe tip surface and zero normal derivative of the pressure $\partial p_a/\partial n = 0$, where $p_0 = \sqrt{P_W\rho_0 c_0/S}$, t is the time, and $S = 3.14 \times 10^{-4}\ \mathrm{m^2}$ is the surface area of the ultrasonic probe tip, (b) sound soft boundary $p_a = 0$ at the liquid/air interface, and (c) hard boundaries at the lateral and bottom sides of the crucible, which is written as:

$$-\frac{1}{\rho_0}(\nabla p_a) = 0 \tag{2}$$

Fig. 1(a) shows the sound distribution along the wave propagation direction z within the liquid alloy at $t = 0$ s. It can be seen clearly that the sound pressure increases with the increase

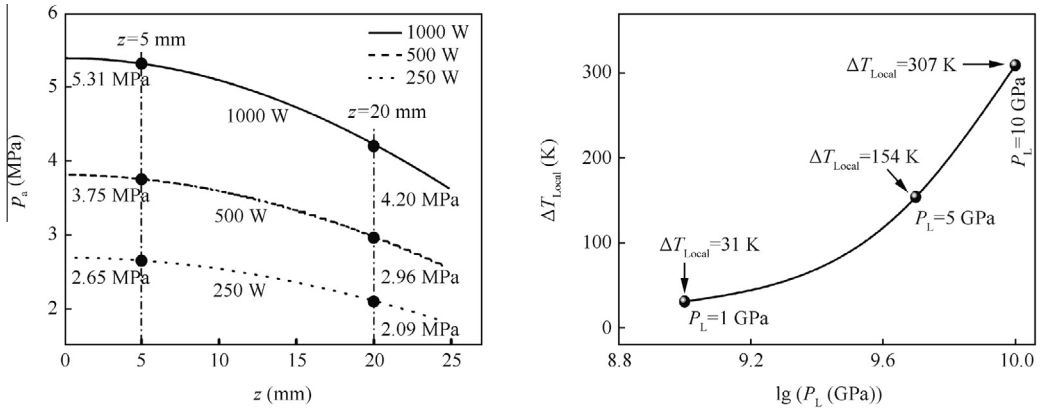

(a) Sound pressure versus propagation distance

(b) Local undercooling versus cavitation sound pressure

Fig. 1 Calculated sound pressure and local undercooling within liquid $Cu_{40}Sn_{45}Sb_{15}$ alloy.

of initial ultrasound power at the ultrasonic probe tip. Moreover, as propagation extends, the sound pressure tends to reduce. In Fig. 1(b), ΔT_{Local} is local undercooling.

3.2. Microstructures formed by ultrasonic solidification

As previously reported,[20] the solidus and liquidus temperatures of ternary $Cu_{40}Sn_{45}Sb_{15}$ alloy are determined to be 509 K and 831 K, and five phase transformations occur successively in the cooling process, which initiates with the formation of primary ε(Cu_3Sn) phase. After this, η(Cu_6Sn_5) and β(SnSb) intermetallic compounds successively nucleate and grow. Finally, the solidification ends with two peri-eutectic transitions of L + β(SnSb) → η(Cu_6Sn_5) + Sn_3Sb_2 and L + Sn_3Sb_2 → η(Cu_6Sn_5) + (Sn).

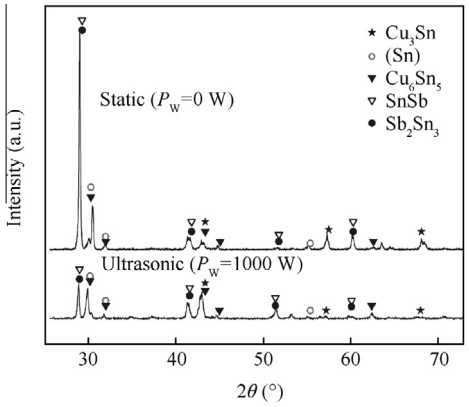

Fig. 2 XRD patterns for ternary $Cu_{40}Sn_{45}Sb_{15}$ alloy solidified under static condition and within ultrasonic field.

In order to investigate the effect of ultrasound on the phase constitution of ternary $Cu_{40}Sn_{45}Sb_{15}$ alloy, the XRD analyses are performed on the solidified samples with various ultrasound powers. Two typical XRD patterns are presented in Fig. 2, which reveal that the solidification microstructures obtained under conventional condition and ultrasound power of 1000 W consist of ε(Cu_3Sn), η(Cu_6Sn_5), β(SnSb), Sn_3Sb_2 and (Sn) phases.

Fig. 3 shows the microstructures of $Cu_{40}Sn_{45}Sb_{15}$ alloy solidified with different ultrasound powers. Under conventional condition (Fig. 3(a)), it can be seen clearly that a large amount of primary ε(Cu_3Sn) phase exists, which grows in faceted way and develops into long coarse strips. The η(Cu_6Sn_5) phase grows into thin layers surrounding primary ε phase. Then, an Sn–Sb intermetallic compound layer grows adjacently to η(Cu_6Sn_5) phase. The EDS analysis indicates that the atomic ratio of Sn:Sb locates between 1 and 1.30. Hence, it is difficult to distinguish β(SnSb) from Sn_3Sb_2 and we call this layer Sn–Sb intermetallic compound. Besides, there are also some (Sn) blocks distributed discontinuously on Sn–Sb intermetallic compound matrix. The parallel growth of the inner primary ε(Cu_3Sn) phase, the η(Cu_6Sn_5) phase and the SnSb phase forms a three-layer lamellar structure.

When ultrasound power of 250 W is applied, as presented in Fig. 3(b), remarkable refinement effect takes place to the primary ε(Cu_3Sn) phase within the whole alloy sample.

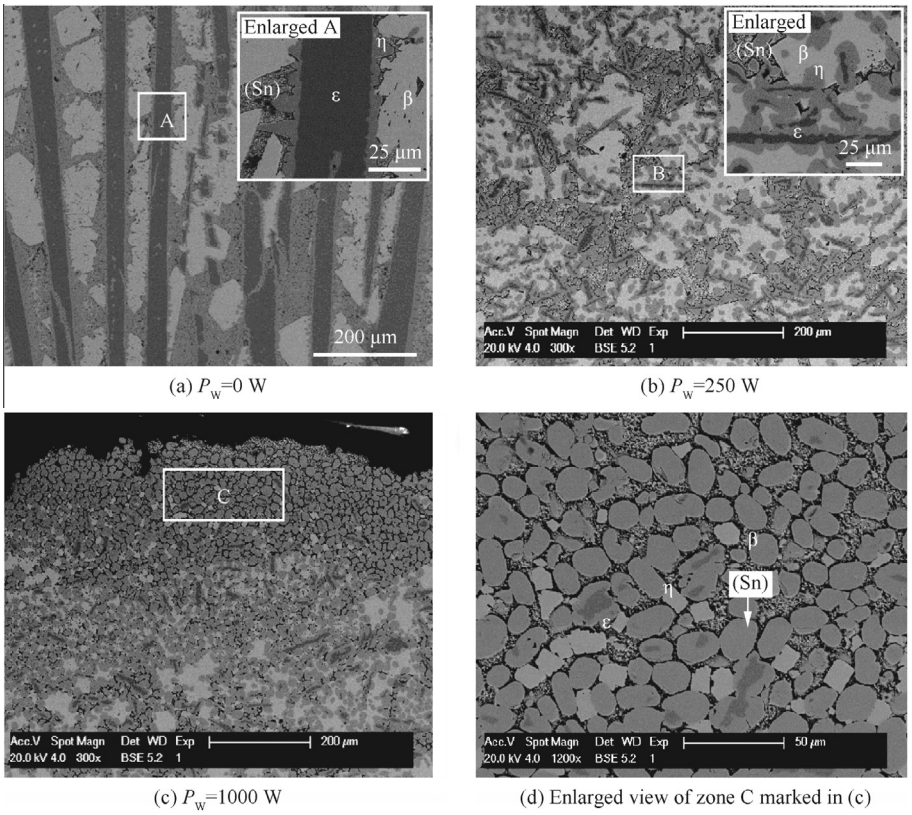

Fig. 3 Solidification microstructures of ternary $Cu_{40}Sn_{45}Sb_{15}$ alloy under various ultrasound power conditions.

Meanwhile, as compared with that during conventional solidification, the thickness of η(Cu_6Sn_5) phase increases. The solidification microstructure formed under ultrasound power 500 W is similar to that under 250 W but seems to be more refined. It also needs to be mentioned that homogeneous microstructure is observed within the alloy samples solidified under ultrasound power of both 250 W and 500 W. However, If the ultrasound power further increases to P_W = 1000 W, as shown in Fig. 3(c), the structure becomes inhomogeneous, and a lot of spherical equiaxed grains appear at the top of the alloy sample. Whereas the similar structure as that in Fig. 3(b) formed in the remaining lower part. This is because the intensive cavitation effect occurs at the sample top when the ultrasound power is sufficiently high. The cavitation leads to the sharply attenuation of the ultrasonic wave at the remaining bottom part of the alloy sample. As seen in the enlarged view of zone C in Fig. 3(d), a large proportion of these equiaxed grains are only made up of η(Cu_6Sn_5) phase, whereas the others are composed of a little amount of primary ε(Cu_3Sn) phase in the core, and the η(Cu_6Sn_5) phase is also the major phase. This is further confirmed by the solute distribution scanning with EDS analysis. As seen in Fig. 4(a) which shows the solute content C, this equiaxed grain is uniform with respect to Cu, Sn and Sb elements distribution, and the atomic ratio of Cu to Sn element is close to 6:5 while about 10 at.% Sb dissolved in the η(Cu_6Sn_5) phase. This demonstrates that such a grain is only composed of η(Cu_6Sn_5) phase without any traces of primary ε(Cu_3Sn) phase. By contrast, as illustrated in Fig. 4(b), there is a little amount of primary ε(Cu_3Sn) phase remaining in the center of the equiaxed grain shown in Fig. 4 (b), whose Sb content is very limited.

3.3. Solidification mechanism within ultrasonic field

On the above mentioned microstructural characteristics, it can be seen clearly that the effect of power ultrasound on the solidification mechanism of ternary $Cu_{40}Sn_{45}Sb_{15}$ alloy lies in the following two aspects. Firstly, it brings about remarkable refinement to the primary ε(Cu_3Sn) phase. Fig. 5 illustrates the relationship between the average size for primary ε(Cu_3Sn) phase versus ultrasound power. As ultrasound power rises, both the length L_ε and width W_ε decrease, and especially for the length, it is decreased from 1135 μm to that of 11 μm under

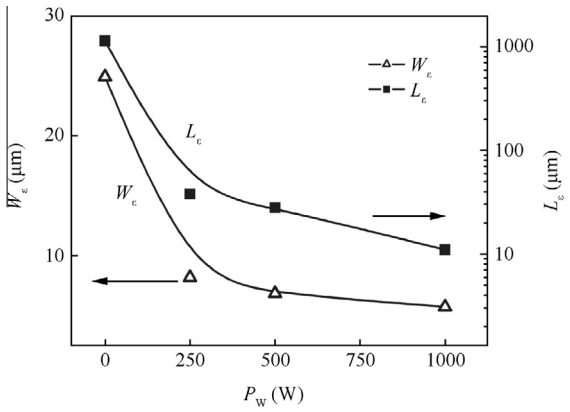

Fig. 5 Average width and length for primary ε(Cu_3Sn) phase.

the ultrasound power of 1000 W, which is reduced by two orders of magnitudes. Meanwhile, the width also declines from 25 μm to that of 6 μm under the highest ultrasound power.

Secondly, the ultrasound may alter the solidification path for ternary $Cu_{40}Sn_{45}Sb_{15}$ alloy. As shown in Fig. 3(c), when the ultrasound is sufficiently intensive, the η(Cu_6Sn_5) phase may directly nucleate and grow from the liquid alloy to form an equiaxed grain in some regions of the alloy melt due to the local intensive cavitation effect. In fact, cavitation effect generates a huge local transient pressure of up to GPa magnitude and affects the nucleation process by elevating the local melting temperature. The change of liquidus temperature T_P with pressure P_L is given by the Clausius–Clapeyron equation as

$$T_P = T_L + T_L \cdot (P_L - P_0) \cdot \Delta V / \Delta H_m \quad (3)$$

where T_L is the liquidus temperature at the atmospheric pressure P_0. ΔV and ΔH_m are the volume change and enthalpy change during liquid–solid transformation, respectively. Assuming that the high pressure P_L in the liquid alloy produced by cavitation effect is up to 1–10 GPa, (Fig. 1(b)), the local undercooling ΔT_{Local} is calculated to be elevated by 30–307 K. The undercooling is sufficient to cool the local alloy melt to a point much lower than the liquidus temperature. In this case, the per-eutectic η(Cu_6Sn_5) phase can nucleate preferentially by preventing the formation of primary ε(Cu_3Sn) phase.

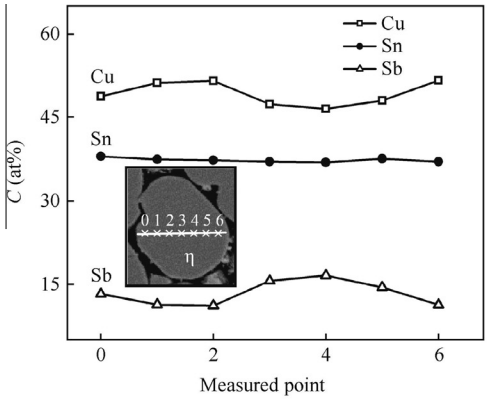

(a) EDS analysis of an equiaxed grain only composed of η phase

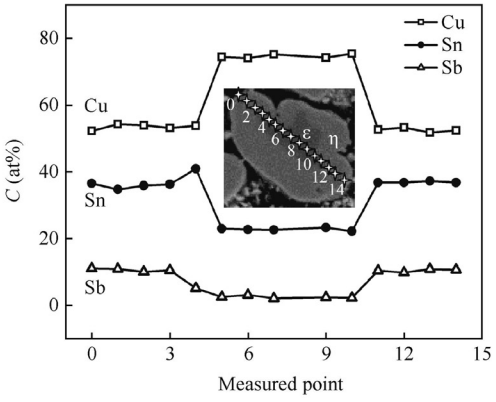

(b) Solute distribution profile of an equiaxed grain consisting of remnant primary ε phase and η phase

Fig. 4 Solute distribution profiles of peri-eutectic structures after high power ultrasonic solidification.

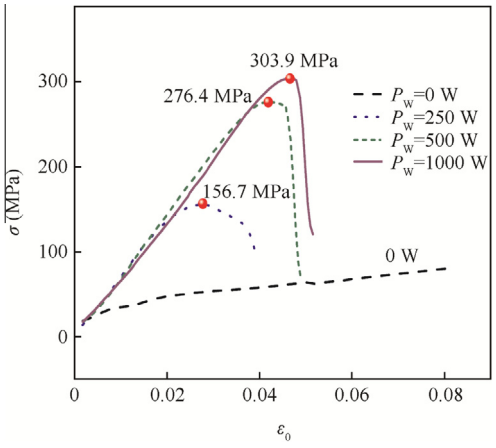

Fig. 6 Stress–strain curve for ternary $Cu_{40}Sn_{45}Sb_{15}$ alloy samples solidified with different ultrasound powers.

3.4. Mechanical property of ultrasonically solidified alloy

Fig. 6 shows the compressive stress–strain curves for ternary $Cu_{40}Sn_{45}Sb_{15}$ alloy samples solidified with different ultrasound powers, in which σ stands for stress and ε_0 denotes strain. Clearly, under conventional condition, the alloy sample sustains a long life without rupture strain, and the corresponding elasticity modulus is 2478 MPa. At a low power ultrasound of 250 W, the compressive strength of the solidified alloy sample is about 156.7 MPa with a fracture strain of 2.7%. As ultrasound power rises, both the compressive strength and fracture strain show an increasing tendency. As seen in Fig. 6, when the ultrasound power reaches the maximum value of 1000 W, the compressive strength rises to 303.9 MPa with a fracture stain of 4.7%, which are 1.94 and 1.74 times higher than those under ultrasound of 250 W, respectively. It also needs to be mentioned that the elasticity modulus also elevates sharply to about 6107 MPa for the ternary $Cu_{40}Sn_{45}Sb_{15}$ alloy samples solidified within ultrasonic field, which is increased by a factor of 2.46 as compared with that during conventional solidification. These results indicate that the introduction of ultrasound during solidification promotes the compressive strength as well as elasticity modulus and decreases the ductility of ternary $Cu_{40}Sn_{45}Sb_{15}$ alloy. The refinement effect on the primary ε (Cu_3Sn) phase and the increase in volume fraction of the η (Cu_6Sn_5) phase take responsibility for the variation in mechanical properties.

4. Conclusions

The effect of power ultrasound on the solidification of ternary $Cu_{40}Sn_{45}Sb_{15}$ peri-eutectic alloy is investigated, which proves that the introduction of power ultrasound is an effective way to control the microstructure formation and promotes the mechanical property for ternary peri-eutectic type alloys. The main conclusions are as follows:

(1) Both of the $Cu_{40}Sn_{45}Sb_{15}$ alloy samples solidified during the conventional condition and within ultrasonic field, are composed of ε(Cu_3Sn), η(Cu_6Sn_5), β(SnSb), Sn_3Sb_2 and (Sn) phases. The introduction of ultrasonic field does not change the phase constitution of this ternary alloy.

(2) The ultrasonic field has a prominent refinement effect on the primary ε(Cu_3Sn) phase, whose size is reduced by nearly two orders of magnitudes as compared with that during conventional solidification.

(3) Under the highest ultrasound power of 1000 W, the intensive cavitation effect at the sample top prevents the formation of primary ε(Cu_3Sn) phase and the η(Cu_6Sn_5) phase nucleates and grows directly from the liquid alloy melt.

(4) The introduction of ultrasound during solidification promotes the compressive strength as well as elasticity modulus and decreases the ductility of ternary $Cu_{40}Sn_{45}Sb_{15}$ alloy.

Acknowledgements

This work was financially supported by the National Natural Science Foundation of China (Nos. 51327901, 51271150 51571164 and 51471134), the Fundamental Research Fund of Northwestern Polytechnical University (No. JCQ01091) of China and the NPU Excellent Personnel Supporting Project of AoXiang New Star of China.

References

1. Chinnama RK, Fauteux C, Neuenschwander J. Evolution of the microstructure of Sn–Ag–Cu solder joints exposed to ultrasonic waves during solidification. *Acta Mater* 2011;**59**(4):1474–8.
2. Zhai W, Hong ZY, Wen XL, Geng DL, Wei B. Microstructural characteristics and mechanical properties of peritectic Cu–Sn alloy within ultrasonic field. *Mater Des* 2015;**72**:43–50.
3. Zhai W, Hong ZY, Mei CX, Wang WL, Wei B. Dynamic solidification mechanism of ternary Ag–Cu–Ge eutectic alloy under ultrasonic condition. *Sci China Ser G-Phys Mech Astron* 2013;**56**(2):462–73.
4. Luque de Castro MD, Priego-Capote F. Ultrasound-assisted crystallization (sonocrystallization). *Ultrason Sonochem* 2007;**14**(6):717–24.
5. Liao Q, Li WP, Liu HC, Zhu LQ. Fabrication of nanostructured electroforming copper layer by means of an ultrasonic-assisted mechanical treatment. *Chin J Aeronaut* 2010;**23**(5):599–603.
6. Ramirez A, Qian M, Davies B, Wilks T, StJohn DH. Potency of high-intensity ultrasonic treatment for grain refinement of magnesium alloys. *Scripta Mater* 2008;**59**(1):19–22.
7. Puga H, Teixeira JC, Barbosa J. The combined effect of melt stirring and ultrasonic agitation on the degassing efficiency of $AlSi_9Cu_3$ alloy. *Mater Lett* 2009;**63**(24–25):2089–92.
8. Khashaba UA, Aljinaidi AA, Hamed MA. Nanofillers modification of Epocast 50–A1/946 epoxy for bonded joints. *Chin J Aeronaut* 2014;**27**(5):1288–300.
9. Zhong G, Wu S, Jiang H, An P. Effects of ultrasonic vibration on the iron-containing intermetallic compounds of high silicon aluminum alloy with 2% Fe. *J Alloys Compd* 2010;**492**(1–2):482–7.
10. Kandemir S, Helen VA, Lawes SDA. Effect of ultrasonic treatment on the microstructure of A201 aluminium alloy for thixoforming. *AIP Conf Proc* 2011;**1353**:1063–8.
11. Li YL, Feng HK, Cao FR, Chen YB, Gong LY. Effect of high density ultrasonic on the microstructure and refining property of Al–5Ti–0.25C grain refiner alloy. *Mater Sci Eng, A* 2008;**487**(1–2):518–23.
12. Wannasin J, Martinez RA, Flemings MC. Grain refinement of an aluminum alloy by introducing gas bubbles during solidification. *Scripta Mater* 2006;**55**(2):115–8.

13. Liu X, Osawa Y, Takamori S, Mukai T. Microstructure and mechanical properties of AZ91 alloy produced with ultrasonic vibration. *Mater Sci Eng, A* 2008;**487**(1–2):120–3.
14. Qian M, Ramirez A, Das A, StJohn DH. The effect of solute on ultrasonic grain refinement of magnesium alloys. *J Cryst Growth* 2010;**312**(15):2267–72.
15. Bantibhai P, Chaudhari GP, Bhingole PP. Microstructural evolution in ultrasonicated AS41 magnesium alloy. *Mater Lett* 2012;**66**(1):335–8.
16. Gao D, Li Z, Han Q, Zhai Q. Effect of ultrasonic power on microstructure and mechanical properties of AZ91 alloy. *Mater Sci Eng, A* 2009;**502**(1–2):2–5.
17. Aghayani MK, Niroumand B. Effects of ultrasonic treatment on microstructure and tensile strength of AZ91 magnesium alloy. *J Alloys Compd* 2011;**509**(1):114–22.
18. Tolnai D, Townsend P, Requena G, Salvo L, Lendvai J, Degischer HP. In situ synchrotron tomographic investigation of the solidification of an AlMg4.7Si8 alloy. *Acta Mater* 2012;**60**(6–7):2568–77.
19. Amberger D, Eisenlohr P, Goken M. On the importance of a connected hard-phase skeleton for the creep resistance of Mg alloys. *Acta Mater* 2012;**60**(5):2277–89.
20. Zhai W, Wang BJ, Lu XY. Rapid solidification mechanism of highly undercooled ternary $Cu_{40}Sn_{45}Sb_{15}$ alloy. *Appl Phys A* 2015;**121**(1):273–81.

Zhai Wei is an associate professor at Northwestern Polytechnical University. Her main research interest is solidification mechanism of liquid alloys within ultrasonic field.

Hong Zhenyu is an associate professor at Northwestern Polytechnical University. His main research interest is acoustic levitation of liquid and solid.

Liu Haiman received the B.S. degree in computational science from Northwest Polytechnical University in 2014, and then became a postgraduate in the same university. She currently studies on the stimulation of sound field and acoustic field in the liquid alloy solidified within ultrasonic field.

Wei Bingbo is a professor at Northwestern Polytechnical University. His main research interest is high undercooling and rapid solidification of liquid alloys.